A general methodology for inverse estimation of the elastic and anelastic properties of anisotropic open-cell porous materials—with application to a melamine foam

Jacques Cuenca, Christophe Van der Kelen, and Peter Göransson

A general methodology for inverse estimation of the elastic and anelastic properties of anisotropic open-cell porous materials—with application to a melamine foam

Jacques Cuenca,[a)] Christophe Van der Kelen, and Peter Göransson
Marcus Wallenberg Laboratory for Sound and Vibration Research, Royal Institute of Technology (KTH), Teknikringen 8, SE-10044 Stockholm, Sweden

This paper proposes an inverse estimation method for the characterisation of the elastic and anelastic properties of the frame of anisotropic open-cell foams used for sound absorption. A model of viscoelasticity based on a fractional differential constitutive equation is used, leading to an augmented Hooke's law in the frequency domain, where the elastic and anelastic phenomena appear as distinctive terms in the stiffness matrix. The parameters of the model are nine orthotropic elastic moduli, three angles of orientation of the material principal directions and three parameters governing the anelastic frequency dependence. The inverse estimation consists in numerically fitting the model on a set of transfer functions extracted from a sample of material. The setup uses a seismic-mass measurement repeated in the three directions of space and is placed in a vacuum chamber in order to remove the air from the pores of the sample. The method allows to reconstruct the full frequency-dependent complex stiffness matrix of the frame of an anisotropic open-cell foam and in particular it provides the frequency of maximum energy dissipation by viscoelastic effects. The characterisation of a melamine foam sample is performed and the relation between the fractional-derivative model and other types of parameterisations of the augmented Hooke's law is discussed. © *2014 AIP Publishing LLC*. [http://dx.doi.org/10.1063/1.4865789]

I. INTRODUCTION

Energy dissipation in fluid-saturated poroelastic materials is governed by the properties of the solid and fluid phases and the interaction between these. Under the modelling paradigm established by Biot,[1–3] it is assumed that the corresponding phenomena are independent and spatially homogeneous at scales and wavelengths much larger than the pore size. According to the ambient conditions, porous materials may thus behave as either solids or equivalent fluids. This has allowed for the development of a vast amount of characterisation methods either focusing on the acoustical or the mechanical properties in order to later include them in a combined model.[4–10] In particular, open-cell foams behave as viscoelastic solids when they are observed under vacuum conditions. This property has been used in the past in order to estimate various properties of the frame of porous materials without the influence of air in the pores.[9,11–13] Alternative methods exist, where the thermal and viscous interactions between the frame and the air in the pores may be neglected at sufficiently low frequencies, providing approximations of the frame parameters.[7,8,10,14]

Previously published works have frequently been restricted to isotropic material modelling. However, porous materials are in general to a certain degree anisotropic in terms of their constitutive properties, either due to the intrinsic geometrical morphology of the microstructure[15–17] or to pre-compression.[18] Despite this, the role of anisotropy in the acoustical and vibrational performance of porous materials is not thoroughly understood. In fact, available characterisation methods assume that the material principal directions[19] are known and aligned with the measurement coordinates.[7,8,20] Recent work on the sensitivity to relative alignment of two anisotropic poro-elastic layers[21] shows that the orientation of the material principal directions of a porous layer dramatically influences its vibroacoustic behaviour. The results therein suggest that deeper knowledge on the behaviour of anisotropic porous materials and the energy dissipation mechanisms manifested in their dynamic behaviour could open new opportunities for the design and optimisation of acoustical treatments.

As observed by several authors,[6,7,11,12,14] the mechanical properties of most foams are frequency-dependent. The available characterisation methods do not explicitly model this frequency dependence, but instead consider the elastic moduli as unknown frequency-dependent complex parameters. This renders the analysis of experimental results difficult and furthermore may provide a non-causal representation of the dynamic behaviour. Work by Pritz[11,12,22,23] and by one of the authors[9,24] shows that a suitable causal model of the viscoelasticity of porous and fibrous materials, may be formulated in terms of an augmented Hooke's law. The augmented Hooke's law[25,26] is a family of models for anelastic[27] (i.e., reversible viscoelastic) materials who share the property that their stiffness matrix may be written as a superposition of a static term and a series of complex valued, frequency-dependent terms accounting for different relaxation phenomena. Two main approaches exist for the parameterisation of the frequency dependence, either in terms of a series of

a)Author to whom correspondence should be addressed. Electronic mail: jcuenca@kth.se

relaxation terms[25,26,28,29] or in terms of a fractional-derivative model.[22,23,30–32] Theoretically equivalent, as shown by Dovstam,[26] both may be used in estimations of the properties of a material through an inverse methodology. Irrespective of the chosen parameterisation, the advantage provided is that the obtained frequency-dependent properties constitute a feasible material model description. Once available, the real and imaginary parts of the moduli may then be extracted a posteriori from such a causal model.

In this paper, a general inverse method for the characterisation of the anisotropic elastic and anelastic properties of the frame of open-cell porous materials is proposed. The basis for the method consists in performing a model fit on a series of measured transfer functions on a sample of foam placed in vacuum in order to remove the influence of the air. Obviously, the number of parameters involved in the material model must be smaller than the number of independently observed states of the material. These data may be ensured through proper choices of either geometrical arrangements, the induced deformation states or the number of frequency lines included, or a combination of these three. Interestingly enough, as illustrated in the current paper, this will be of a lesser concern for real materials where the lack of material symmetry naturally renders the measured transfer functions independent *per se*.

The starting point for the present paper is the recent work by the authors,[33] where the proposed approach was validated against data from an artificial (numerical) simplified experiment in the special case of an orthotropic material with the principal coordinates aligned with the coordinate system of the experimental setup. Simulating a seismic-mass setup[11] in vacuum, a set of vibration transfer functions were extracted for a cubic material sample. Due to the assumed material property symmetry and the cubic geometry chosen, an asymmetric seismic mass was used. It was shown that the material properties could be estimated within a maximum relative error of 5%, the largest deviations observed for the Poisson's ratios.

Several authors have reported that due to the foaming processes used, most foams are transversely isotropic or close to orthotropic.[7,8,10] However, to the knowledge of the authors, no attempt has been made to identify the deviation of the natural coordinates of the material from the measurement coordinates. In order to generalise the previously published results, the orientations of the material principal directions of orthotropy are here included as unknown parameters in the inverse estimation. The material model relies on a fractional differential equation, yielding an augmented Hooke's law in the frequency domain, where the orthotropic elastic and anelastic properties appear distinctively in the stiffness matrix. The method is comprehensive in that it allows for the estimation of the complete dynamic Hooke's tensor of the frame of an open-cell foam, including the three angles that determine the orientation of the material principal directions of orthotropy. An important aspect is that no *a priori* knowledge about the material is required.

The model and methodology are here illustrated on a melamine foam, which is widely used as a sound-absorbing material and has been studied using Biot's theory.[4,7,18] In addition to providing a satisfactory fit between measured and predicted transfer functions, it is also demonstrated that alternative parameterisations of the frequency dependence of the material properties may be derived from the present model.

II. MODEL OF THE MATERIAL

A. Constitutive equation

The constitutive law for the frame of the porous material *in vacuo* may be derived as a special case of Biot's equations for anisotropic porous materials.[1,2] Indeed, considering a porous material with zero pressure and displacement in the fluid phase yields the constitutive equation for the frame in the form of a Hooke's law.

A large variety of existing models may be used to account for the dynamic effects in the motion of the frame. Here, an augmented Hooke's law[25,26] is used, which provides a causal representation of the stiffness matrix of the material as a linear superposition of an elastic part, accounting for the frequency-independent fully relaxed state of the material, and an anelastic part, accounting for frequency-dependent reversible viscoelastic deformation. In the original form of the augmented Hooke's law,[25] the anelastic part of the stiffness matrix is expressed as a series where each term represents a different relaxation process of the material. Such parameterisation has been used to characterise solid and porous materials[9,29,34,35] and presents the advantage of providing a direct physical interpretation to each term of the series. Nevertheless, for a given material the number of parameters to be estimated is large, an aspect which potentially can cause practical computational difficulties.

Alternative parameterisations of the augmented Hooke's law using a fractional derivative approach[30–32,36] have been used in the case of solid and polymeric damping materials.[22,23] For the present purposes, this representation is interesting as it allows for a model of the relaxation behaviour with a reduced number of parameters[26] and a corresponding reduction of the computational load.

In the present paper, the fractional differential equation proposed by Caputo and Mainardi[31,32] is used. In the case of an anisotropic material, the constitutive equation can be written, using shortened matrix notation, as

$$\left(1 + \frac{\partial^\alpha}{\partial(t/\tau)^\alpha}\right)\sigma_i(t) = \left(C_{ij} + M_{ij}\frac{\partial^\alpha}{\partial(t/\tau)^\alpha}\right)\varepsilon_j(t), \quad (1)$$

where σ_i and ε_j denote the components of the stress and strain tensors as

$$\boldsymbol{\sigma} = \begin{bmatrix} \sigma_{11} & \sigma_{22} & \sigma_{33} & \sigma_{23} & \sigma_{31} & \sigma_{12} \end{bmatrix}^{\mathrm{T}}, \quad (2)$$

$$\boldsymbol{\varepsilon} = \begin{bmatrix} \varepsilon_{11} & \varepsilon_{22} & \varepsilon_{33} & 2\varepsilon_{23} & 2\varepsilon_{31} & 2\varepsilon_{12} \end{bmatrix}^{\mathrm{T}}, \quad (3)$$

C_{ij} denote the components of the fully relaxed stiffness matrix, M_{ij} denote the components of a suitable memory mechanism matrix, τ is the relaxation time of the material, in seconds, and α is the fractional derivative order. The fractional derivative order assumes a value within the range

$$0 < \alpha \leq 1, \tag{4}$$

with $\alpha = 1$ corresponding to the limiting case of a Zener model.[32] It is worth noting that the definition of the relaxation time in the case of a fractional derivative model differs from the usual definition for an exponential decay. As a matter of fact, the solution of an equation of the type of Eq. (1) is given by a Mittag-Leffler power-law function in the time domain,[32] which in the limiting case $\alpha = 1$ simplifies to an exponential function.

Introducing the variable change

$$M_{ij} = C_{ij} + B_{ij}, \tag{5}$$

together with application of the Laplace transform to Eq. (1) leads to the augmented Hooke's law in the frequency domain

$$\sigma_i(\omega) = H_{ij}(\omega)\varepsilon_j(\omega), \tag{6}$$

where $\omega = 2\pi f$ is the circular frequency and the components of the frequency-dependent stiffness matrix are given by

$$H_{ij}(\omega) = C_{ij} + \frac{B_{ij}(i\omega/\beta)^\alpha}{1 + (i\omega/\beta)^\alpha}, \tag{7}$$

with $\beta = 1/\tau$ denoting the relaxation frequency in rad · s^{-1}. The stiffness matrix thus obtained provides a model of the deformation of the material as a superposition of its fully relaxed state and a complex frequency-dependent relaxation phenomenon. In general, a given material may present different types of anisotropy in the elastic and anelastic phenomena. However, both phenomena share the same microstructural geometry and therefore it is assumed for the purposes of the present paper that the elastic and anelastic parts of the stiffness matrix are collinear, by stating that

$$B_{ij} = b\,C_{ij}, \tag{8}$$

where b is a real scalar constant. The final form of the stiffness matrix is then

$$H_{ij}(\omega) = C_{ij}\left(1 + \frac{b(i\omega/\beta)^\alpha}{1 + (i\omega/\beta)^\alpha}\right). \tag{9}$$

Obviously, this is a rather far reaching hypothesis, the validity of which depends on the type of the constituent solid frame material involved. For the specific melamine foam studied in Sec. IV, the results show that it is a fair assumption. Future studies on other types of materials are however required to deduce its general applicability.

B. Model of the anisotropy and physical constraints

In the natural coordinate system of the material, denoted (x_0, y_0, z_0), the elastic part of the stiffness matrix has the symmetric form[19]

$$\mathbf{C}^0 = \begin{bmatrix} \frac{1}{E_1} & -\frac{\nu_{21}}{E_2} & -\frac{\nu_{13}}{E_1} & 0 & 0 & 0 \\ & \frac{1}{E_2} & -\frac{\nu_{32}}{E_3} & 0 & 0 & 0 \\ & & \frac{1}{E_3} & 0 & 0 & 0 \\ & & & \frac{1}{G_{23}} & 0 & 0 \\ & & & & \frac{1}{G_{31}} & 0 \\ & \text{(sym)} & & & & \frac{1}{G_{12}} \end{bmatrix}^{-1}, \tag{10}$$

where E_i is the Young's modulus along axis i, G_{ij} is the shear modulus in plane (i, j), and ν_{ij} is the Poisson's ratio for extension along i resulting in contraction along j. According to the 2nd law of thermodynamics, the stiffness matrix must be positive-definite, imposing restrictions on the moduli, given by[19]

$$E_i > 0, \quad G_{ij} > 0, \quad \nu_{ij}^2 < E_i/E_j,$$
$$2\nu_{21}\nu_{32}\nu_{13} < 1 - \nu_{21}^2 E_1/E_2 - \nu_{32}^2 E_2/E_3 - \nu_{13}^2 E_3/E_1. \tag{11}$$

C. Transformation of coordinates

Matrix $\mathbf{C}^0$ must be expressed in the coordinate system in which the measurements and the model are set up, denoted (x, y, z). Using the natural coordinate system of the material as a reference, this is achieved by application of a coordinate transformation to $\mathbf{C}^0$, consisting of a composition of three successive rotations. Using extrinsic rotations with Tait-Bryan angles[37] (ϕ_1, ϕ_2, ϕ_3) around the original fixed axes (x_0, y_0, z_0) as a convention, the transformation is defined by the rotation matrix

$$\mathbf{a} = \mathbf{a}_z\mathbf{a}_y\mathbf{a}_x = \begin{bmatrix} a_{11} & a_{12} & a_{13} \\ a_{12} & a_{22} & a_{23} \\ a_{13} & a_{23} & a_{33} \end{bmatrix}, \tag{12}$$

where

$$\mathbf{a}_x = \begin{bmatrix} 1 & 0 & 0 \\ 0 & \cos\phi_1 & \sin\phi_1 \\ 0 & -\sin\phi_1 & \cos\phi_1 \end{bmatrix}, \quad \mathbf{a}_y = \begin{bmatrix} \cos\phi_2 & 0 & -\sin\phi_2 \\ 0 & 1 & 0 \\ \sin\phi_2 & 0 & \cos\phi_2 \end{bmatrix},$$

$$\mathbf{a}_z = \begin{bmatrix} \cos\phi_3 & \sin\phi_3 & 0 \\ -\sin\phi_3 & \cos\phi_3 & 0 \\ 0 & 0 & 1 \end{bmatrix}. \tag{13}$$

In order for the rotation matrix to be uniquely defined in terms of the rotation angles, these are defined as

$$\phi_1 \in [-\pi, \pi], \quad \phi_2 \in [-\pi/2, \pi/2], \quad \phi_3 \in [-\pi, \pi]. \tag{14}$$

The material elasticity in the measurement coordinate system is then described by the stiffness matrix

$$\mathbf{C} = \mathbf{A}\mathbf{C}^0\mathbf{A}^{\mathrm{T}}, \tag{15}$$

where the Bond matrix $\mathbf{A}$ is obtained from $\mathbf{a}$ as[27]

$$
\mathbf{A} = \begin{bmatrix}
a_{11}^2 & a_{12}^2 & a_{13}^2 & 2a_{12}a_{13} \\
a_{21}^2 & a_{22}^2 & a_{23}^2 & 2a_{22}a_{23} \\
a_{31}^2 & a_{32}^2 & a_{33}^2 & 2a_{32}a_{33} \\
a_{21}a_{31} & a_{22}a_{32} & a_{23}a_{33} & a_{22}a_{33}+a_{23}a_{32} \\
a_{11}a_{31} & a_{12}a_{32} & a_{13}a_{33} & a_{12}a_{33}+a_{13}a_{32} \\
a_{11}a_{21} & a_{12}a_{22} & a_{13}a_{23} & a_{12}a_{23}+a_{13}a_{22}
\end{bmatrix}
$$

$$
\begin{bmatrix}
2a_{11}a_{13} & 2a_{11}a_{12} \\
2a_{21}a_{23} & 2a_{21}a_{22} \\
2a_{31}a_{33} & 2a_{31}a_{32} \\
a_{21}a_{33}+a_{23}a_{31} & a_{21}a_{32}+a_{22}a_{31} \\
a_{11}a_{33}+a_{13}a_{31} & a_{11}a_{32}+a_{12}a_{31} \\
a_{11}a_{23}+a_{13}a_{21} & a_{11}a_{22}+a_{12}a_{21}
\end{bmatrix} \quad (16)
$$

D. Isotropic reference and degree of anisotropy

In the general case, the moduli that characterise a certain material may differ by orders of magnitude. While this poses no theoretical problems, it is more convenient for the inverse estimation procedure proposed here to replace them with non-dimensional parameters. The material model is then reformulated in terms of the elastic properties of an arbitrary isotropic material of reference and a set of scaling constants. These may be interpreted as the degree of anisotropy of the material in each of its moduli, with respect to the arbitrary isotropic reference material. The isotropic reference is then used as the starting point for the inverse estimation procedure, which then consists in finding the scaling constants as a deviation from this reference.

The isotropic reference material is characterised by its elastic properties E_0 and ν_0 and its anelastic properties α_0, β_0, and b_0. The scaling constants are defined as the ratio between each material property and the corresponding one for the isotropic reference, as

$$
\begin{aligned}
&\xi_i = E_i/E_0, \quad i = 1,2,3, \\
&\xi_i = G_{kl}/G_0, \quad i = 9-k-l = 4,5,6, \\
&\xi_i = \nu_{kl}/\nu_0, \quad i = 4+k+l = 7,8,9, \\
&\xi_{10} = \alpha/\alpha_0, \quad \xi_{11} = \beta/\beta_0, \quad \xi_{12} = b/b_0,
\end{aligned} \quad (17)
$$

where $G_0 = E_0/2(1+\nu_0)$ is the shear modulus of the isotropic reference material. The stiffness matrix in the natural coordinate system then assumes the form

$$
\mathbf{C}^0 = \begin{bmatrix}
\dfrac{1}{\xi_1 E_0} & -\dfrac{\xi_7 \nu_0}{\xi_2 E_0} & -\dfrac{\xi_8 \nu_0}{\xi_1 E_0} & 0 & 0 & 0 \\
& \dfrac{1}{\xi_2 E_0} & -\dfrac{\xi_9 \nu_0}{\xi_3 E_0} & 0 & 0 & 0 \\
& & \dfrac{1}{\xi_3 E_0} & 0 & 0 & 0 \\
& & & \dfrac{1}{\xi_4 G_0} & 0 & 0 \\
& \text{(sym)} & & & \dfrac{1}{\xi_5 G_0} & 0 \\
& & & & & \dfrac{1}{\xi_6 G_0}
\end{bmatrix}^{-1} .
$$

$$(18)$$

Rewriting the requirements determined by Eqs. (4) and (11) in terms of the scaling constants and considering the constraints on the properties of the isotropic material of reference yield the constraints for the 12 scaling constants as

$$
\begin{aligned}
&E_0 > 0, \quad -1 < \nu_0 < 1/2, \\
&\xi_i > 0, \quad i = 1, \ldots, 6, \\
&\xi_{4+i+j}^2 \nu_0^2 < \xi_i/\xi_j, \quad ij = 21, 13, 32, \\
&2\nu_0^3 \xi_7 \xi_8 \xi_9 < 1 - \nu_0^2 \left(\xi_7^2 \xi_1/\xi_2 + \xi_8^2 \xi_3/\xi_1 + \xi_9^2 \xi_2/\xi_3 \right), \\
&0 < \xi_{10} \le 1/\alpha_0, \quad \xi_{11} > 0, \quad \xi_{12} > 0,
\end{aligned}
$$

$$(19)$$

with $\xi_i = 1$ $(i = 1, \ldots, 12)$ corresponding to the isotropic reference.

The nine scaling constants of the orthotropic model, the three scaling constants of the anelastic properties and the three angles (ϕ_1, ϕ_2, ϕ_3) are then the unknowns to be determined from measurements using the proposed inverse estimation method.

III. INVERSE ESTIMATION METHOD

A. Optimisation problem

With the assumed material symmetries, together with the proportionality between elastic and anelastic moduli as discussed above, the model used here has 15 material properties to be estimated: 9 elastic moduli for the orthotropic material symmetry, 3 angles defining the orientation of the principal directions, and 3 anelastic parameters. Thus, given an arbitrarily chosen isotropic reference as discussed above, determined by parameters E_0, ν_0, α_0, β_0, and b_0, the set of parameters to estimate is composed of 12 scaling constants and 3 angles, which for the present purposes are gathered in the form of a column matrix

$$
\mathbf{x} = [\xi_1\, \xi_2\, \xi_3\, \xi_4\, \xi_5\, \xi_6\, \xi_7\, \xi_8\, \xi_9\, \xi_{10}\, \xi_{11}\, \xi_{12}\, \phi_1\, \phi_2\, \phi_3]^{\mathrm{T}}. \quad (20)
$$

Hence, $\mathbf{x}$ defines a 15-dimensional space in which the model evolves. The properties of a given material are then defined as the set $\mathbf{x}_0$ that minimises a distance in such space between the model and the experiment.

In the current work, the estimation of the properties of the material is formulated as an optimisation problem in which the distance to minimise defines the objective function. Assuming that M transfer functions are extracted from the measurement and replicated using the model with a certain set of parameters $\mathbf{x}$, the objective function is defined as

$$
d(\mathbf{x}) = 1 + \sum_{m=1}^{M} \sum_{n=1}^{N} \left| \frac{u_m(\omega_n, \mathbf{x}) - u_m^{(\exp)}(\omega_n)}{u_m^{(\exp)}(\omega_n)} \right|^2, \quad (21)
$$

where N is the number of frequency points of each transfer function, and $u_m^{(\exp)}$ and u_m, respectively, denote the experimental and simulated transfer functions. The objective function, formulated in terms of a relative difference, gives equal

importance to all frequency samples in the transfer functions. Furthermore, it should be noted in Eq. (21) that a constant is added to the objective function as a general precaution in order to prevent numerical issues for small values.

Formally, the optimisation problem consists in minimising Eq. (21) subjected to the constraints in Eq. (19).

It is important to stress that the material properties to be estimated are independent from frequency and that all frequency lines in the transfer functions are simultaneously taken into account within the objective function. This ensures that the number of experimental data values available for the inverse estimation is significantly larger than the number of parameters to estimate.

B. Experimental setup

The experimental setup, chosen for the present material characterisation, consists of a cubic sample of porous material placed between a vertically vibrating plate and a seismic loading, as depicted in Fig. 1. The setup is placed in a vacuum chamber in order to remove the air from the pores of the material and the mass of the seismic loading is chosen so as to enforce variations of the transfer functions within the frequency range of interest. In order for the setup to reveal the full anisotropy of the sample, 4 acceleration transfer functions are measured between the shaker and laser vibrometer points $\mathbf{r}_i$ $(i = 1,\ldots,4)$ in each of the 3 directions of space, for a total of 12 transfer functions. Note that, in contrast to previous work by the authors,[33] the seismic mass is uniform. This choice is made based on the fact that in general, for real porous materials exhibiting a significant degree of anisotropy and also having natural coordinates unaligned with the measurement directions, enough deviation from symmetry is met to provide independent observations of the state of the material under these conditions.

The laser vibrometer provides the vertical displacement at the 4 points $\mathbf{r}_i$ and thus gives access to 3 degrees of freedom of the seismic loading, i.e., vertical translation and two out-of-plane rotations. Therefore, 9 independent experimental data values are available at each frequency, which is appropriate considering the orthotropic symmetry of the stiffness matrix. It is then required that the transfer functions contain at least two frequencies in order to extract the 15 material properties. As detailed in the application in Sec. IV,
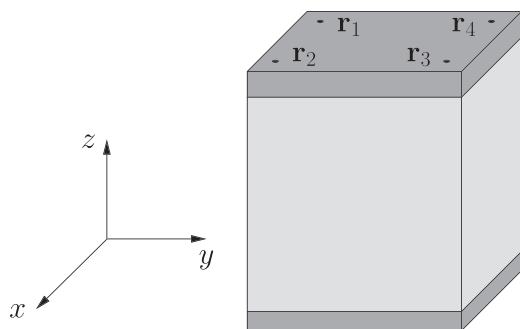

FIG. 1. Schematic view of the experimental setup. $\mathbf{r}_i$, laser vibrometer points for displacement measurement.

the measurement is performed at a large number of frequencies in order to minimise the estimation error.

The coordinate system used for the inverse estimation is the coordinate system (x, y, z) attached to the sample. In practice, the sample is rotated so that its x, y, and z directions are subsequently aligned with the direction of excitation. As a convention, the orientation of Fig. 1, with a vertical z direction is considered as a reference, and a rotation of $\pi/2$ around the y axis (respectively, $-\pi/2$ around the x axis) is applied to align the x axis (respectively, y axis) with the vertical direction, using the transformation of Sec. II C.

C. Numerical implementation

The set of 12 transfer functions extracted from the experimental setup must be replicated using the model in order to build the objective function. Here, they are numerically simulated using a conventional finite element model of the setup including the sample, the shaker plate, and the seismic mass. A uniform harmonic force is imposed on the bottom face of the shaker plate and homogeneous natural boundary conditions are used elsewhere in order to account for vacuum conditions. Furthermore, the contact between the three substructures is considered to be perfect with no lateral sliding, i.e., continuity of all displacements and velocities is assumed at the interfaces. The specific numerical aspects of the finite element implementation are adapted to the material to characterise and thus are detailed in the application example in the next section.

The optimisation problem is implemented using the globally convergent method of moving asymptotes.[38] The latter is based on the approximation of the objective function by a convex variable-separated function of the optimisation variables $\mathbf{x}$ where vertical asymptotes determine the interval of admissibility of each variable at the successive iterations. The present paper explores the advantage embedded in conservative convex separable approximations, particularly suited to problems with a large number of unknowns. The finite element model is included within the optimiser as a subroutine providing the transfer functions, where the stiffness matrix of the material is updated at each iteration. The algorithm is considered to have converged to an optimal solution if both the objective function and the optimisation variables, normalised to unity, vary less than 10^{-3} in 3 successive iterations.

A numerical validation has been performed through testing of the method against a range of fictitious materials, analogous to previous work.[33] While the results will not be detailed here, the conclusions are that for a material with a significant degree of anisotropy and whose natural coordinates are not aligned with the measurement directions, the transfer functions are differentiable by using a symmetrical mass loading.

IV. CHARACTERISATION OF A MELAMINE FOAM

A. Preparation of the setup

Melamine open-cell foams are widely used for sound insulation and absorption. They are obtained by foaming a melamine-formaldehyde precondensate by heating.[39] Due to

the nature of the foaming process, there exists a rising direction which is close to the vertical direction and whose properties are susceptible to differ from the other two directions, thereby motivating the existence of transversely isotropic or orthotropic symmetry. For the foam specimen used herein, the z axis of the coordinate system attached to the sample is chosen as the foam rising direction reported by the manufacturer of the material. It is commercially manufactured and therefore other details about the final properties of the foam are not known.[18]

Specific precautions are required in order to prepare the samples for the measurements. In the present case, in order to avoid non-linearity in the vibrations due to detachments, the foam was bonded to the bottom plate and the seismic mass (Fig. 1) using adhesive tape. Therefore, three different samples were used, one for the measurement corresponding to each spatial coordinate orientation. The samples were cut from a large block of melamine foam, where they were adjacent to each other, covering a maximum distance of 30 cm. It is henceforth assumed that the spatial homogeneity of the material is ensured over that distance and therefore the dispersion in the estimated material properties due to spatial inhomogeneity cannot be quantified here.

The mass densities of the samples and the loading masses present slight differences, which needs to be taken into account in the numerical model. The samples are 10 cm-side cubic and their mass density is, respectively, 9.1 kg m^{-3}, 10.2 kg m^{-3}, and 9.5 kg m^{-3} for the measurements along the x, y, and z directions. The seismic masses are balsa plates of 10 cm $\times$ 10 cm $\times$ 2 cm including an added mass of 7.45 g by the adhesive tape. The total mass densities ρ_s of the seismic loadings are, respectively, 177.25 kg m^{-3}, 169.75 kg m^{-3}, and 216.75 kg m^{-3} for the measurements along the x, y, and z directions. For the three samples, the bottom support is a Plexiglas plate of 10 cm $\times$ 10 cm $\times$ 0.792 cm.

The 12 transfer functions are measured in the frequency range 0–400 Hz with a resolution of 0.1563 Hz, using an accelerometer on the bottom plate and a laser vibrometer on the seismic mass. In order to reduce the computational cost when numerically reproducing the transfer functions, the data are limited to 76 uniformly spaced frequency lines within the range 70.625–398.75 Hz, with a resolution of 4.375 Hz. Therefore, a total of 912 experimental data values are available, from which 684 are independent from each other (see Sec. III B).

B. Validation of vacuum conditions

In the measurements performed, vacuum conditions were supposed to have been reached if the static pressure inside the vacuum chamber was lower than 3% of the atmospheric pressure, that is, below 3 kPa, which corresponds to a medium range vacuum.[40] This was achieved by means of a pump and monitored using a vacuum gauge. Due to the existence of flow resistivity in the porous material,[1] it is necessary to wait a sufficiently long time for the vacuum to be settled inside the sample. In order to determine the stabilisation time of the vacuum conditions, the evolution of the transfer functions used for the inverse estimation was
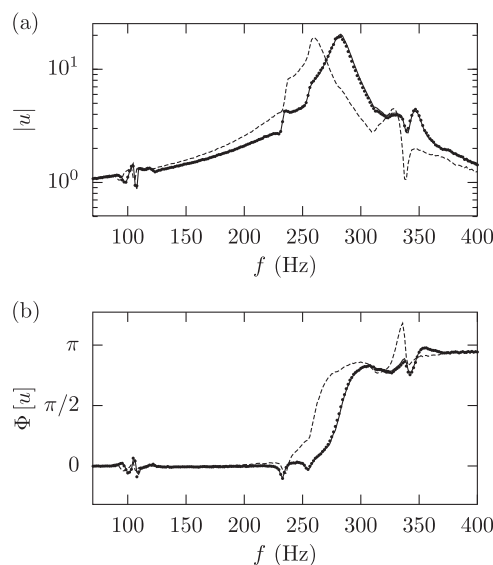

FIG. 2. Modulus (a) and phase (b) of a transfer function of the setup after different times in the vacuum chamber. Dashed line, at ambient atmospheric pressure; solid line, after 8 hours below 3 kPa; dotted line, after 24 hours below 3 kPa.

observed. Figure 2 shows one of the transfer functions at ambient pressure conditions and after 8 and 24 hours at less than 3 kPa. The mean absolute variation of the transfer functions between 8 and 24 hours in the vacuum chamber is 3.05%. It is thus concluded that the vacuum conditions were stable after 8 hours in the vacuum chamber, and therefore subsequent measurements were performed under such conditions. It is worth noting that the seismic mass used for the results in Fig. 2 is lighter than the one used for the inverse estimations later on.

C. Finite element model

The finite element model is called iteratively within the optimiser and thus it is necessary to reduce its computational cost by minimising the spatial resolution of the finite element mesh. Preliminary investigations show that the Young's moduli of the melamine foam to be characterised are higher than 100 kPa. The minimum values of the compressional and shear wavelengths[27] estimated at a frequency above the frequency range of interest, namely 500 Hz, using an isotropic solid model with the highest mass density measured and a Poisson's ratio ranging from -1 to 0.5, are $\lambda_C = 6.32$ m for compressional waves and $\lambda_s = 3.65$ m for shear waves. The dimensions of the sample are thus considerably smaller than the wavelength and therefore the requirement for the mesh is that it correctly represents the different types of motion inside the material. Thus, a mesh with two elements per side of the sample was used, with quadratic order Lagrange polynomial tetrahedral elements.[41]

D. Model fit and estimated properties

The application of the method to the melamine foam specimen requires an isotropic material of reference as a starting point. The estimation procedure was repeated using several isotropic materials as initial configurations and it was

verified that the resulting estimations were equivalent in terms of the estimated parameters. To illustrate the inverse estimation, one particular choice of isotropic material of reference is shown below. The properties are chosen as

$$E_0 = 3 \cdot 10^5 \, \text{Pa}, \quad \nu_0 = 0.3,$$
$$\beta_0 = 832.16 \, \text{krad} \cdot \text{s}^{-1}, \quad \alpha_0 = 0.7, \quad b_0 = 0.3. \tag{22}$$

The optimisation variables are initially at the neutral state where the material is isotropic and the material natural coordinates are aligned with the measurement coordinates, which is given by

$$\xi_i = 1, \quad i = 1, \dots, 12,$$
$$\xi_i = 0, \quad i = 13, 14, 15. \tag{23}$$

The objective function converges after 155 iterations within the tolerance described in Sec. III C. Figure 3 shows the transfer functions between the reference at the bottom plate and top-plate point $\mathbf{r}_1$, obtained experimentally and by the inverse estimation method. It is observed that the current experimental setup allows to differentiate all transfer functions and therefore an asymmetrical seismic loading is not required for the present material.

The resulting optimal set of variables $\mathbf{x}$ yields the estimated properties shown in Table I. The precision of the estimated material properties is not accessible in a direct manner due to the fact that the method consists in an inverse estimation. Nevertheless, previous results[33] indicate that the method provides the different terms of the estimated stiffness matrix with an uncertainty of 0.5% to 5%. The estimated material properties are therefore given here with 3 significant figures. Furthermore, the angles (ϕ_1, ϕ_2, ϕ_3) obtained from the inverse estimation determine the natural coordinate

TABLE I. Estimated properties of the melamine foam.

Property	Value	Unit
E_1	448	kPa
E_2	211	kPa
E_3	170	kPa
G_{23}	104	kPa
G_{31}	124	kPa
G_{12}	101	kPa
ν_{21}	0.445	-
ν_{13}	−0.514	-
ν_{32}	0.433	-
β	813	krad/s
α	0.333	-
b	0.296	-
ϕ_1	−0.118	rad
ϕ_2	0.030	rad
ϕ_3	0.131	rad

system of the material, shown together with the measurement coordinate system in Fig. 4.

Finally, the full frequency-dependent complex stiffness matrix of the melamine foam frame is obtained from Eq. (9) using the estimated properties and is shown in Fig. 5 in the natural coordinate system. Note that the stiffness matrix terms have been extrapolated beyond the frequency range accessible from the measurements in order to illustrate the loss factor peak and inflexion of the stiffness at the relaxation frequency.

E. Discussion

It can be observed in Fig. 3 that the transfer functions obtained by the proposed method are reasonably close to the experimental ones. In particular, the model accurately accounts for the compressional phenomena and transverse coupling in the deformation of the material, which respectively correspond to the main peak and secondary variations of the transfer functions. Moreover, a direct correspondence is observed between the frequency of the main peak of the transfer functions and the value of the Young's moduli in the three directions of space reported in Table I.
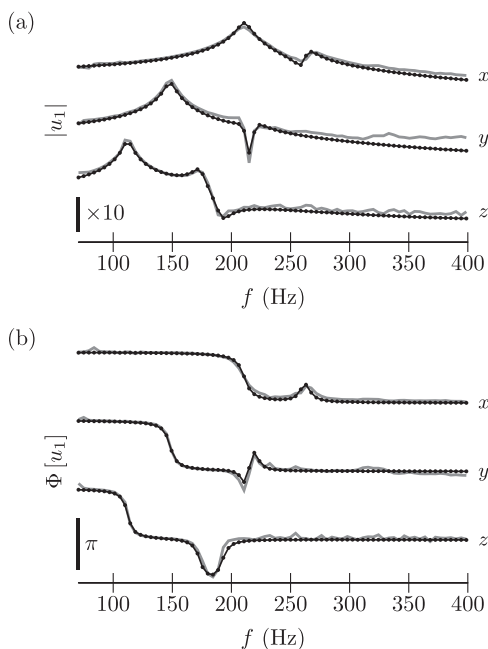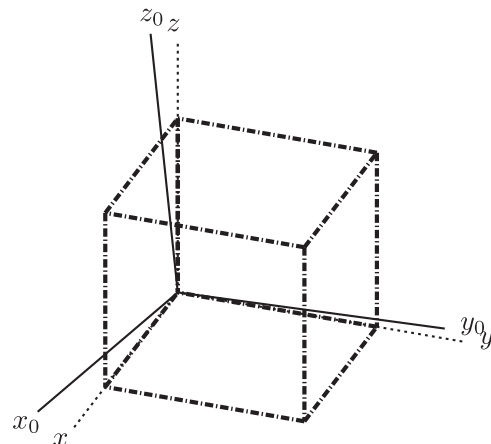

FIG. 3. Modulus (a) and phase (b) of the transfer functions between the reference at the bottom plate and point $\mathbf{r}_1$ of the top plate, for the three spatial orientations of the sample. Grey solid line, experiment; black dotted line, model.

FIG. 4. Cubic sample of foam in the measurement coordinate system (x, y, z) and estimated natural coordinate system (x_0, y_0, z_0).
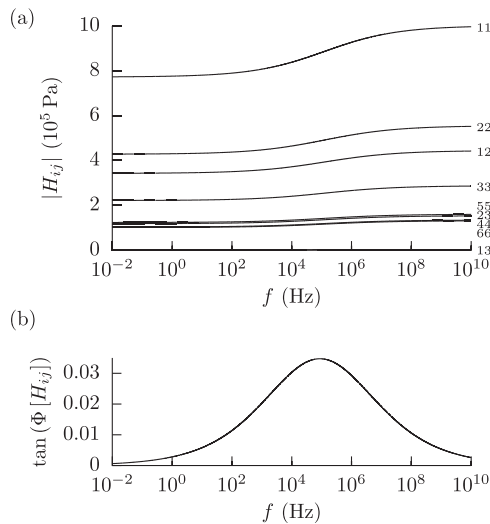
FIG. 5. Frequency-dependent stiffness matrix of the frame of the melamine foam from estimated parameters, in the natural coordinate system. (a) Modulus of the different terms of the stiffness matrix; (b) loss factor.

The extracted set of material properties satisfies the constraints given by Eqs. (4) and (11), which guarantees that the material model is a feasible realisation. Furthermore, the natural coordinate system obtained exhibits a low deviation from the measurement coordinates, which is consistent with the fact that the foam rising direction is aligned with one of the measurement coordinates, namely, the z axis. In this regard, it is observed that the lowest Young's modulus is E_3, which at first sight contradicts the common case where the rising direction exhibits the highest compressional stiffness.[16] However, for the present material, this is most probably due to compression in the z direction which is coupled with compression in the x direction via a negative Poisson's ratio ν_{13}.

It can be observed in Fig. 5 that the different terms of the stiffness matrix of the frame of the melamine foam present the well-known frequency dependence of the stiffness of viscoelastic materials predicted by the present type of constitutive equation.[22,31,32] Indeed, the modulus of the different terms of the stiffness matrix increases with frequency and the phase presents a peak which corresponds to maximum energy loss by anelastic effects. Moreover, the frequency of the damping peak is lower than the relaxation frequency and depends on the fractional derivative order that characterises the material.[22] In this case, the maximum loss factor is reached at a frequency of 129.393 kHz. It is important to stress that, while a maximum loss at such a frequency does not have a direct significance for the present application, it characterises the frequency-dependent properties of the polymer, regardless of its microstructural arrangement.[12,42]

The results obtained emphasise the importance of considering the orientation of the material principal directions as an unknown property of the material. Indeed, the secondary variations of the transfer functions measured using this type of setup are due to transverse coupling between the different directions of motion of the material. In the present case, although the angles separating the measurement and natural coordinate systems are small, they are nevertheless

responsible for the appearance of the secondary variations in the transfer functions.

V. ALTERNATIVE PARAMETERISATIONS

A. Frequency-dependent moduli

A common practice is to estimate the anisotropic moduli of a material as frequency-dependent quantities.[6–8,11,12,14] The properties estimated herein can be presented in such an alternative manner, by considering that the anelastic frequency dependence is contained in the Young's moduli, shear moduli, and Poisson ratios themselves. Such equivalent frequency-dependent moduli are obtained by expanding Eq. (9) and identifying it in the form of Eq. (10) and represented in Fig. 6. This type of parameterisation highlights an important property of the present model. In fact, the Young's and shear moduli carry the complex frequency dependence, while the Poisson's ratios are necessarily real and constant. This is an intrinsic consequence of the assumed proportionality in the material model.

This result is consistent with previous work by Jaouen *et al.*[7] on a melamine foam. The results therein show that the Young's and shear moduli increase with frequency and the imaginary part of the shear moduli exhibits the characteristic viscoelastic peak. Additionally, in the same paper, one of the Poisson's ratios was reported to be close to a constant real value of 0.44 over a limited frequency range. Results by Sahraoui *et al.*[14] corroborate these trends on foams assumed to be isotropic.
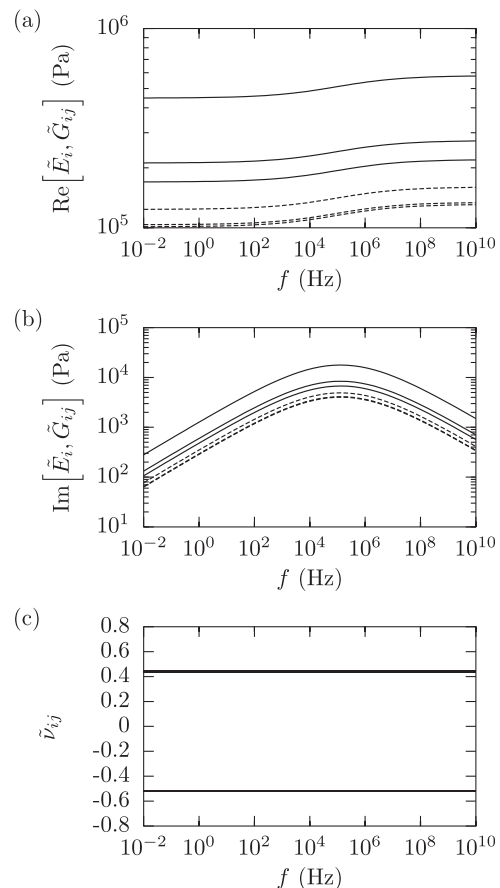

FIG. 6. Equivalent frequency-dependent material moduli. Real (a) and imaginary (b) parts of $\tilde{E}_i$ (solid line) and $\tilde{G}_{ij}$ (dashed line). (c) $\tilde{\nu}_{ij}$.

B. Discrete-process and continuous-spectrum relaxation models

The fractional-derivative model used in the present paper is one of the possible parameterisations of the augmented Hooke's law and has been preferred here for its inherently reduced number of parameters. Other parameterisations include discrete-process relaxation models and continuous-spectrum relaxation models.[26] In particular, previous work makes extensive use of discrete processes,[9,24,29,34,35] which presents the advantage that each process corresponds to a separate relaxation phenomenon in the form of an exponential decay in the time domain. As pointed out by Dovstam,[26] all parameterisations are valid and equivalent as long as they closely simulate the experimental data in the frequency range of interest. In order to link the present results to previous works, alternative discrete-process and continuous-spectrum parameterisations for the melamine foam from the estimated parameters of the fractional-derivative model are calculated.

A material relaxation function may be defined as the frequency-dependent factor of the stiffness matrix, which for the fractional-derivative model assumes the form

$$R_f(\omega) = 1 + \frac{b\,(i\omega/\beta)^\alpha}{1 + (i\omega/\beta)^\alpha}. \qquad (24)$$

The relaxation functions for the discrete-process and continuous-spectrum relaxation models are, respectively,[26]

$$R_d(\omega) = 1 + \sum_{n=1}^{N} \frac{b_n\,i\omega/\beta_n}{1 + i\omega/\beta_n} \qquad (25)$$

and

$$R_c(\omega) = 1 + \int \frac{\tilde{b}(\tilde{\beta})\,i\omega/\tilde{\beta}}{1 + i\omega/\tilde{\beta}}\,d\tilde{\beta}. \qquad (26)$$

The fractional-derivative model is governed by 3 parameters, α, β, and b, the discrete-process model is governed by N pairs (b_n, β_n), and the continuous model is governed by a continuous spectrum $b(\beta)$.
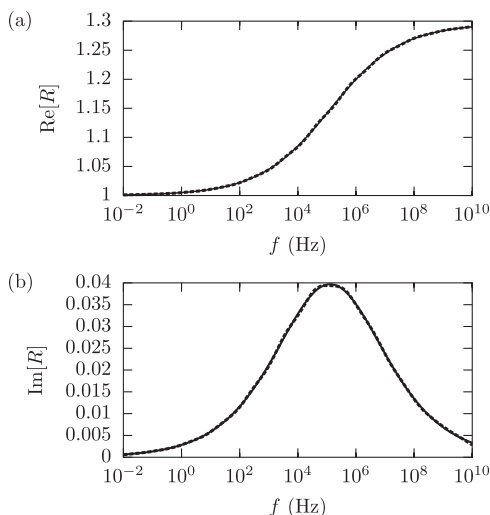

FIG. 7. Discrete process fit of the relaxation function. (a) Real part; (b) imaginary part. Solid line, fractional-derivative model; dashed line, discrete-process model using 12 processes.
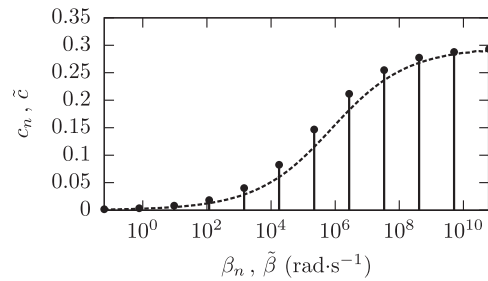

FIG. 8. Relaxation spectrum. Bullet points, discrete-process model; dashed line, continuous-spectrum model.

A discrete-process model for the melamine foam may be obtained by fitting Eq. (25) onto Eq. (24) in a least-squares sense. Figure 7 shows such a fit using a prescribed set of 12 logarithmically distributed relaxation frequencies β_n from $2\pi \cdot 10^{-2}$ to $2\pi \cdot 10^{10}$. The resulting b_n are the amplitudes of the different relaxation processes and their individual values depend on the number of processes in the parameterisation. The cumulative sum c_n of the amplitudes b_n is therefore chosen as an invariant representation of the spectrum, shown in Fig. 8 for the present material.

The knowledge of the discrete-process parameterisation in the frequency domain allows for the time-domain relaxation function to be computed as[26]

$$r_d(t) = \sum_n b_n e^{-t/\tau_n}, \qquad (27)$$

where $\tau_n = 1/\beta_n$ are the relaxation times of the different processes. Figure 9 shows the predicted time-domain relaxation function for the melamine foam.

Further on, the relaxation function according to the continuous-spectrum model may be derived also, as an approximation using a large number of discrete processes. Using 384 processes, the relaxation function indistinguishably fits the fractional-derivative relaxation function of Fig. 7, with the corresponding spectrum $\tilde{c}$ represented as a dashed line in Fig. 8. Accordingly, the time relaxation function $r_c(t)$ is computed and represented with a dashed line in Fig. 9.

The ability to simulate the time relaxation function at longer times depends on the distribution of the discrete relaxation frequencies in the low frequency range. Figure 9 illustrates this, as the decay is overestimated due to the lack of terms with larger relaxation times. In the present case, this is overcome by including lower relaxation frequencies in the discrete-process model fitting.
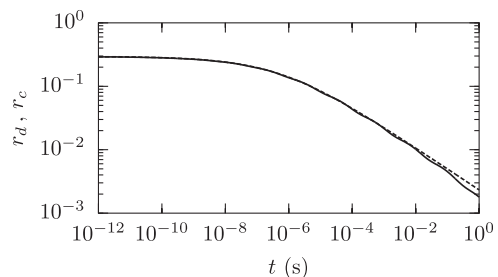

FIG. 9. Relaxation function in the time domain. Solid line, discrete-process model; dashed line, continuous-spectrum model.

In that sense, it is important to stress that the different parameterisations are not necessarily unique and that, in the case of the melamine foam here characterised, the frequency dependence of the stiffness matrix has been obtained from data in a limited frequency range available experimentally.

VI. CONCLUSION

The present paper proposes a model of the elastic and anelastic properties of the frame of anisotropic open-cell porous materials and an inverse method for their experimental characterisation.

The results suggest that the proposed constitutive law, based on a fractional-derivative augmented Hooke's law, is an appropriate model for the anisotropic complex frequency-dependent stiffness matrix of open-cell foams. It has been shown, by applying the method to a sample of melamine foam, that such material can be successfully modelled using the proposed model in the frequency range of interest.

It is important to stress that the parameterisation of the augmented Hooke's law is not unique. In the present case, the feasibility of the approach has been shown using a fractional-derivative formulation, chosen for its reduced number of parameters. It has been shown that various equivalent parameterisations of the augmented Hooke's law may be used, each of them revealing different aspects of the material properties. For instance, a parameterisation in terms of frequency-dependent moduli shows that the Young's and shear moduli carry the complex frequency dependence while the Poisson's ratios are real and constant. In addition, descriptions in terms of discrete or continuous relaxation processes give a straightforward interpretation of the material anelasticity as a time-domain relaxation phenomenon. These parameterisations are straightforwardly derived from the fractional-derivative model, thus making the connection with previous work.[7,9,14,24,29,34,35]

Another important aspect is that the present model relies on the strong simplifying assumption that the elastic and anelastic properties obey to the same material symmetry. Also, due to the microstructure of the foam, the relaxation mechanisms are most certainly different for compression and shear. A combined methodology is in current development in order to remove this assumption, where the elastic properties are determined using a static inverse estimation method,[5] allowing the present method to be used to determine the separate anisotropic anelastic properties.

A key aspect of the application of the method is the degree of symmetry in the sample to characterise within the experimental setup as a whole. Previous work by the authors[33] suggests the use of an asymmetrical seismic mass in order to make the setup more sensitive to shear in the special case of a material whose natural coordinates are aligned with the measurement coordinates and whose degree of anisotropy is weak, namely, a nearly transversely isotropic material. The present results indicate that an asymmetrical seismic mass is not required in the case of a real material such as the one investigated here, where the natural and measurement coordinate systems differ and where the degree of anisotropy is sufficiently high to introduce differences

among the individual transfer functions. Whether or not the symmetry in the setup must be broken in order to identify the parameters of a specific material must be decided on a case-specific basis. A means to provide insight into this aspect is to inspect the measured transfer functions and their frequency dependence in order to assess their degree of mutual independence.

The inverse estimation procedure proposed herein may be adapted to more specific or more general cases. For instance, the method can in principle be generalised to the case of materials whose relaxation and retardation times are different,[22] which however increases the number of parameters to estimate. Also, a more general type of anisotropy may be considered but may require a modification of the experimental protocol due to the fact that the current setup provides 9 independent experimental values at each frequency, which is appropriate for orthotropic materials. Further research would therefore be needed in this direction.

The present approach finds immediate use in numerical models of the acoustics of anisotropic porous materials such as, for instance, the weak formulation of Biot's equations and its finite element implementation developed by Hörlin and Göransson.[43] The stiffness matrix of the frame and the anisotropic flow resistivity tensor are among the input parameters of such formulation, the latter being accessible via a recently developed experimental methodology.[4]

[1]M. A. Biot, "Mechanics of deformation and acoustic propagation in porous media," J. Appl. Phys. **33**(4), 1482–1498 (1962).

[2]M. A. Biot, "Generalized theory of acoustic propagation in porous dissipative media," J. Acoust. Soc. Am. **34**(9), 1254–1264 (1962).

[3]M. A. Biot, "Theory of deformation of a porous viscoelastic anisotropic solid," J. Appl. Phys. **27**(5), 459–467 (1956).

[4]C. Van der Kelen and P. Göransson, "Identification of the full anisotropic flow resistivity tensor for multiple glass wool and melamine foam samples," J. Acoust. Soc. Am. **134**(6), 4659–4669 (2013).

[5]C. Van der Kelen, J. Cuenca, and P. Göransson, "A method for characterisation of the static elastic properties of the porous frame of orthotropic open-cell foams," Int. J. Eng. Sci. (submitted).

[6]M. Etchessahar, S. Sahraoui, L. Benyahia, and J. F. Tassin, "Frequency dependence of elastic properties of acoustic foams," J. Acoust. Soc. Am. **117**(3), 1114–1121 (2005).

[7]L. Jaouen, A. Renault, and M. Deverge, "Elastic and damping characterizations of acoustical porous materials: Available experimental methods and applications to a melamine foam," Appl. Acoust. **69**(12), 1129–1140 (2008).

[8]M. Melon, E. Mariez, C. Ayrault, and S. Sahraoui, "Acoustical and mechanical characterization of anisotropic open-cell foams," J. Acoust. Soc. Am. **104**, 2622 (1998).

[9]H. J. Rice and P. Göransson, "A dynamical model of light fibrous materials," Int. J. Mech. Sci. **41**(4–5), 561–579 (1999).

[10]S. Sahraoui, E. Mariez, and M. Etchessahar, "Linear elastic properties of anisotropic open-cell foams," J. Acoust. Soc. Am. **110**, 635 (2001).

[11]T. Pritz, "Frequency dependence of frame dynamic characteristics of mineral and glass wool materials," J. Sound. Vib. **106**(3), 161–169 (1986).

[12]T. Pritz, "Dynamic Young's modulus and loss factor of plastic foams for impact sound isolation," J. Sound. Vib. **178**(3), 315–322 (1994).

[13]A. Sfaoui, "On the viscoelasticity of the polyurethane foam," J. Acoust. Soc. Am. **97**(2), 1046–1052 (1995).

[14]S. Sahraoui, E. Mariez, and M. Etchessahar, "Mechanical testing of polymeric foams at low frequency," Polym. Test. **20**(1), 93–96 (2000).

[15]A. T. Huber and L. J. Gibson, "Anisotropy of foams," J. Mater. Sci. **23**(8), 3031–3040 (1988).

[16]L. J. Gibson and M. F. Ashby, *Cellular Solids: Structure and Properties*, Cambridge Solid State Science Series (Cambridge University Press, 1999).

[17]W. E. Warren and A. M. Kraynik, "The linear elastic properties of open-cell foams," J. Appl. Mech. **55**(2), 341–346 (1988).

[18]A. Geslain, O. Dazel, J.-P. Groby, S. Sahraoui, and W. Lauriks, "Influence of static compression on mechanical parameters of acoustic foams," J. Acoust. Soc. Am. **130**(2), 818–825 (2011).

[19]R. M. Jones, *Mechanics of Composite Materials* (Taylor & Francis, Philadelphia, 1999), 519 p.

[20]M. Barbagallo, "Statistical energy analysis and variational principles for the prediction of sound transmission in multilayered structures," Ph.D. thesis, Royal Institute of Technology (KTH), 2013. Trita-AVE 2013:04.

[21]E. Lind Nordgren, P. Goransson, J.-F. Deu, and O. Dazel, "Vibroacoustic response sensitivity due to relative alignment of two anisotropic poroelastic layers," J. Acoust. Soc. Am. **133**(5), EL426–EL430 (2013).

[22]T. Pritz, "Analysis of four-parameter fractional derivative model of real solid materials," J. Sound. Vib. **195**, 103–115 (1996).

[23]T. Pritz, "Five-parameter fractional derivative model for polymeric damping materials," J. Sound. Vib. **265**, 935–952 (2003).

[24]P. Göransson, "Acoustic and vibrational damping in porous solids," Philos. Trans. R. Soc. London, Ser. A **364**(1838), 89–108 (2006).

[25]K. Dovstam, "Augmented Hooke's law in frequency domain. A three dimensional, material damping formulation," Int. J. Solids Struct. **32**(19), 2835–2852 (1995).

[26]K. Dovstam, "Augmented Hooke's law based on alternative stress relaxation models," Comput. Mech. **26**(1), 90–103 (2000).

[27]J. M. Carcione, *Wave Fields in Real Media: Wave Propagation in Anisotropic, Anelastic and Porous Media* (Elsevier, 2001).

[28]M. A. Biot, "Theory of stress-strain relations in anisotropic viscoelasticity and relaxation phenomena," J. Appl. Phys. **25**(11), 1385–1391 (1954).

[29]M. Dalenbring, "Experimental material damping estimation for planar isotropic laminate structures," Int. J. Solids Struct. **39**(19), 5053–5079 (2002).

[30]R. L. Bagley and P. J. Torvik, "A theoretical basis for the application of fractional calculus to viscoelasticity," J. Rheol. **27**, 201 (1983).

[31]M. Caputo and F. Mainardi, "A new dissipation model based on memory mechanism," Pure Appl. Geophys. **91**(1), 134–147 (1971).

[32]M. Caputo and F. Mainardi, "Linear models of dissipation in anelastic solids," Riv. Nuovo Cimento **1**(2), 161–198 (1971).

[33]J. Cuenca and P. Göransson, "Inverse estimation of the elastic and anelastic properties of the porous frame of anisotropic open-cell foams," J. Acoust. Soc. Am. **132**(2), 621–629 (2012).

[34]M. Dalenbring, "Damping function estimation based on measured vibration frequency responses and finite-element displacement modes," Mech. Syst. Signal. Process. **13**(4), 547–569 (1999).

[35]M. Dalenbring, "Validation of estimated isotropic viscoelastic material properties and vibration response prediction," J. Sound. Vib. **265**(2), 269–287 (2003).

[36]R. L. Bagley and P. J. Torvik, "Fractional calculus—A different approach to the analysis of viscoelastically damped structures," AIAA J. **21**, 741–748 (1983).

[37]J. C. Samin and P. Fisette, *Symbolic Modeling of Multibody Systems, Solid Mechanics and Its Applications* (Springer, 2003).

[38]K. Svanberg, "A class of globally convergent optimization methods based on conservative convex separable approximations," SIAM J. Optimiz. **12**(2), 555 (2002).

[39]H. Mahnke, G. Kreibiehl, H. Weber, and F. P. Woerner, "Manufacture of resilient foams based on a melamine-formaldehyde condensate," U.S. patent 4334971 (1982).

[40]V. V. Rao, T. B. Ghosh, and K. L. Chopra, *Vacuum Science and Technology* (Allied Publishers Ltd, 1998).

[41]Y. Fung and P. Tong, *Classical and Computational Solid Mechanics*, Advanced Series in Engineering Science (World Scientific, 2001).

[42]N. C. Hilyard, *Mechanics of Cellular Plastics* (Macmillan, 1982).

[43]N. E. Hörlin and P. Göransson, "Weak, anisotropic symmetric formulations of Biot's equations for vibro-acoustic modelling of porous elastic materials," Int. J. Numer. Meth. Eng. **84**(12), 1519–1540 (2010).